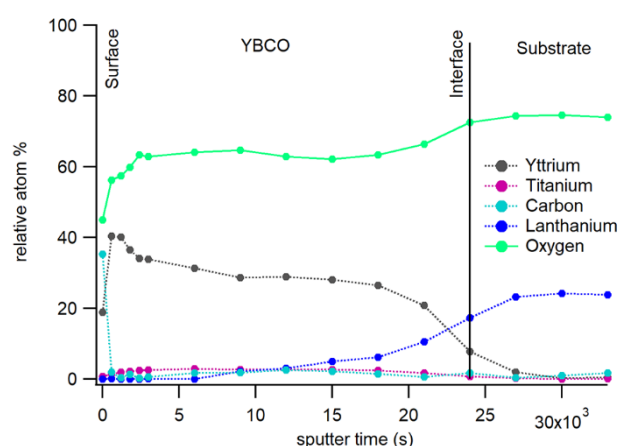


## Supplementary information

### Evaluation of nanoparticle distribution in solution-derived $\text{YBa}_2\text{Cu}_3\text{O}_{7-\delta}$ nanocomposite thin films by XPS depth profiling in combination with TEM analysis.

Els Bruneel, Hannes Rijckaert, Javier Diez Sierra, Klaartje De Buysser and Isabel Van Driessche

Ghent University, Department of Chemistry, Sol-Gel Centre for Research on Inorganic Powders and Thin Films Synthesis (SCRiPTS), Krijgslaan 281-S3, 9000 Ghent, Belgium;



**Figure S1:** Depth profile of pyrolyzed 15 mol-%  $\text{SrTiO}_3$ -added YBCO nanocomposite film on an  $\text{LaAlO}_3$  substrate, including the oxygen signal

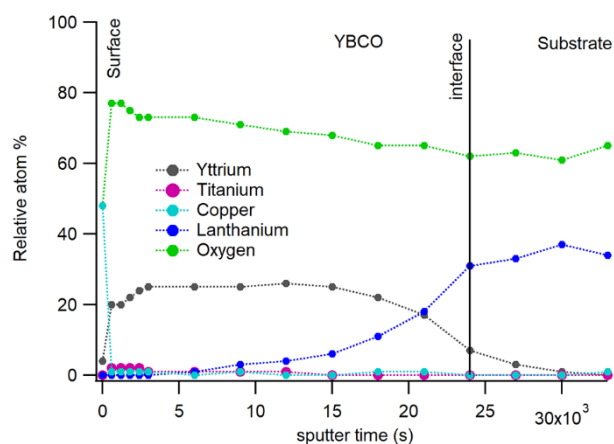


**Figure S2:** Depth profile of crystallized 10 mol-%  $\text{SrTiO}_3$ -added YBCO nanocomposite film on an  $\text{LaAlO}_3$  substrate, including the oxygen signal

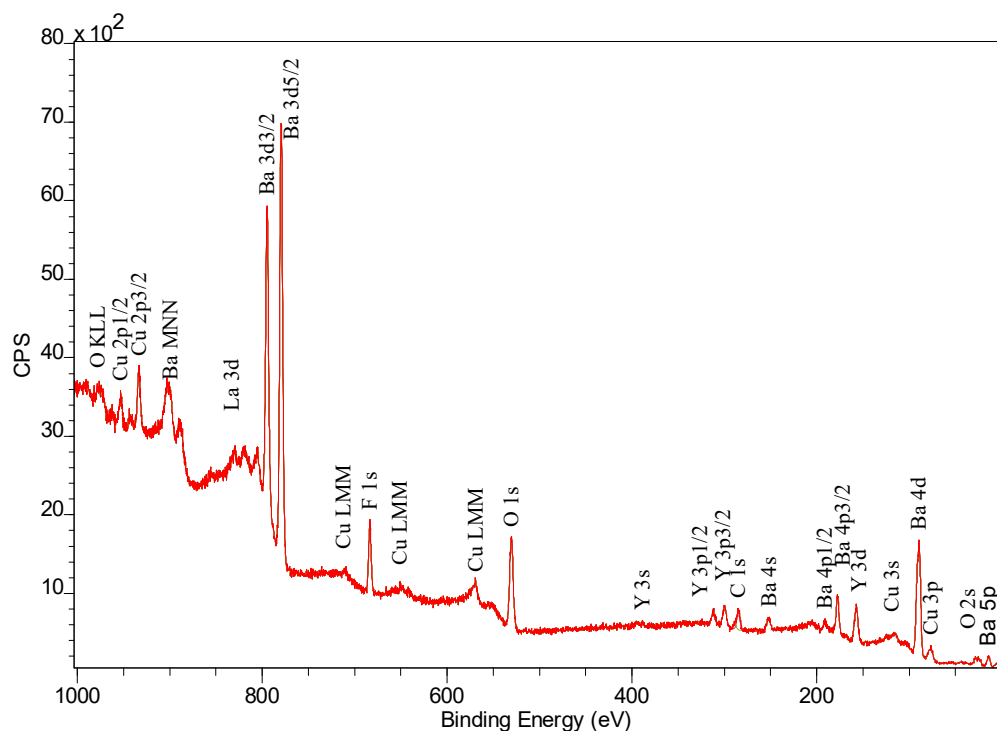


**Figure S3:** Survey of the surface of a crystallized 10 mol-%  $\text{ZrO}_2$ -added YBCO nanocomposite film on an  $\text{LaAlO}_3$  substrate

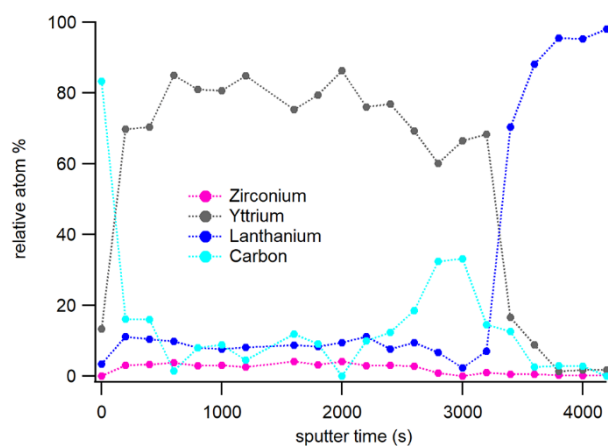


**Figure S4:** Depth profile of crystallized 10 mol-%  $\text{ZrO}_2$ -added YBCO nanocomposite film on an  $\text{LaAlO}_3$  substrate.

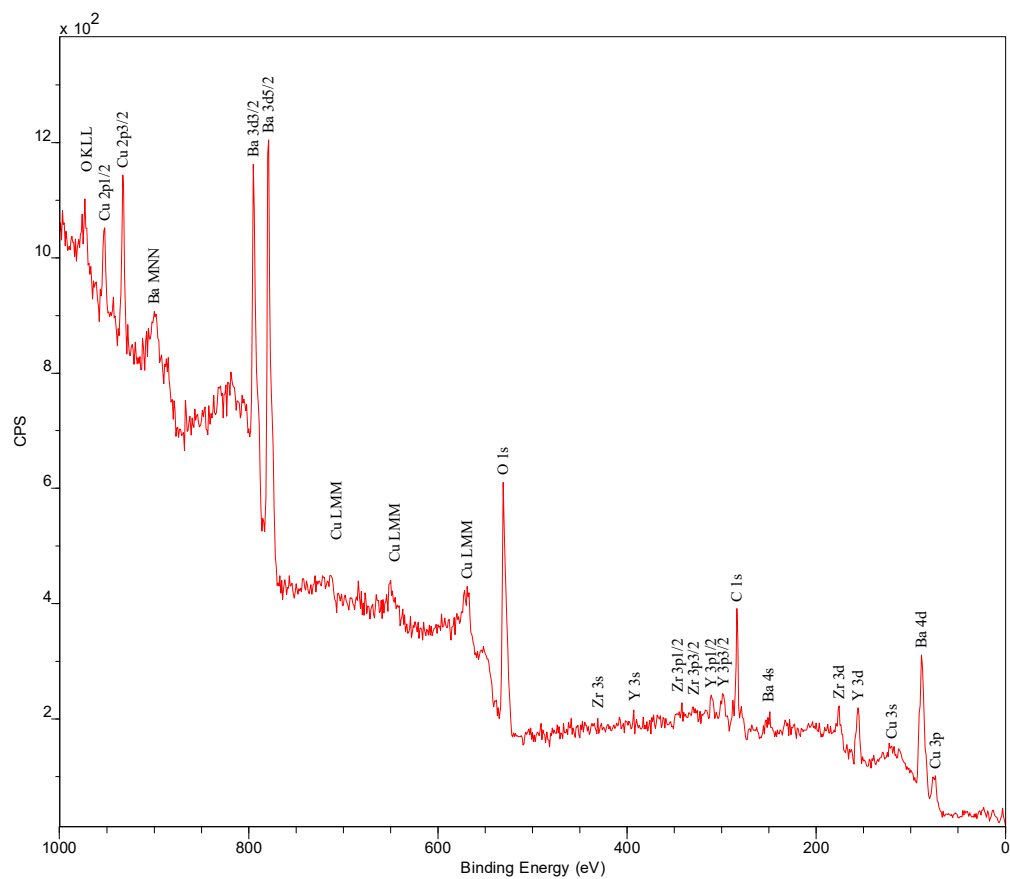


**Figure S5:** Survey of the surface of crystallized 10 mol-%  $\text{ZrO}_2$ -added YBCO nanocomposite film on an  $\text{LaAlO}_3$  substrate

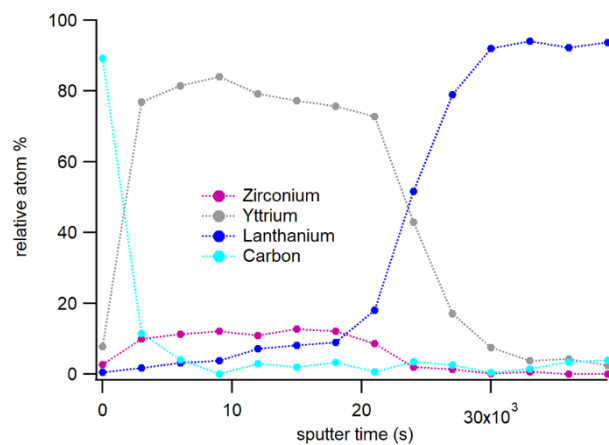


**Figure S6:** Depth profile of crystallized 10 mol-%  $\text{ZrO}_2$ -added YBCO nanocomposite film on an  $\text{LaAlO}_3$  substrate

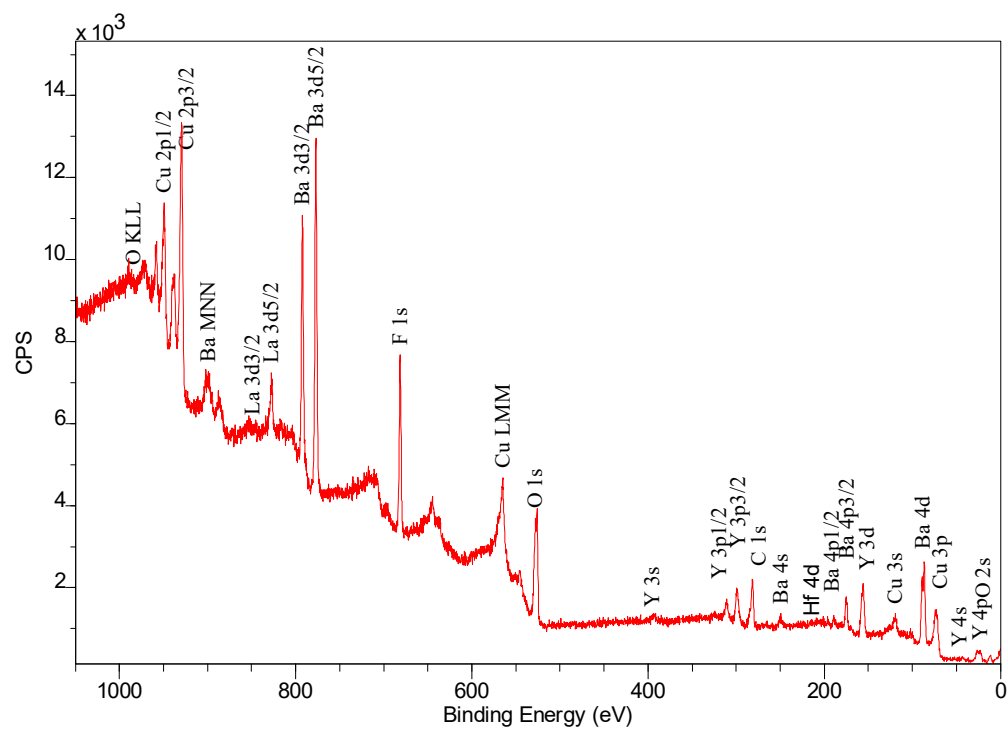


**Figure S7:** Survey of the surface of pyrolyzed 7.5 mol-% HfO<sub>2</sub>-added YBCO nanocomposite film on an LaAlO<sub>3</sub> substrate.

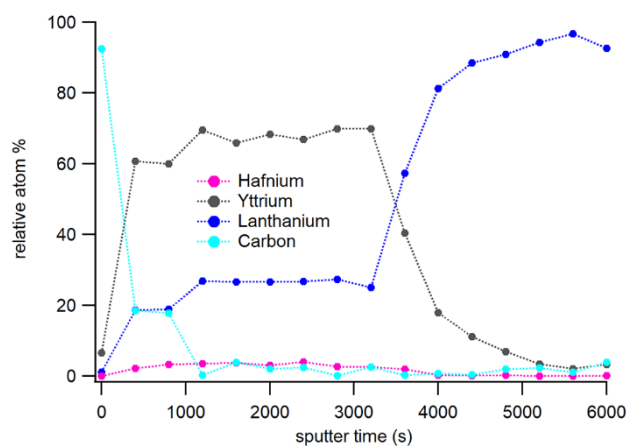


**Figure S8:** Depth profile of pyrolyzed 7.5mol-% HfO<sub>2</sub>-added YBCO nanocomposite film on an LaAlO<sub>3</sub> substrate

The superconducting properties of SrTiO<sub>3</sub>-added YBCO nanocomposite films were measured inductively via THEVA Cryoscan™ with the voltage criterion of 50  $\mu$ V. It can be concluded that self-field  $J_c$  values at 77 K (Table S1) are slightly decreased in relation to an increased volume of SrTiO<sub>3</sub> nanoparticles.

**Table S1:** Critical current density ( $J_c$ ) of 0, 5, 10 and 15 mol-% SrTiO<sub>3</sub>-added YBCO films on an LaAlO<sub>3</sub> substrate, calculated via inductively measurements.

STO nanoparticles mol-%	$J_{c,av}$ (0 T, 77 K) MA cm <sup>-2</sup>
0	4.4
5	4.1
10	3.9
15	3.6

To investigate the influence of SrTiO<sub>3</sub> nanoparticles in the YBCO matrix, YBCO with 0, 5 and 10 mol-% SrTiO<sub>3</sub> nanoparticles on LaAlO<sub>3</sub> substrates are coated with silver (1 micron) via lithography and laser-cut to nano-bridges of  $\sim$ 15-20  $\mu$ m width and 800  $\mu$ m length for the transport measurements via Physical Property Measurement System with  $E_c = 1 \mu$ V cm<sup>-1</sup>. Figure S9a shows the magnetic field dependence of the critical current density at 77 K and  $H//c$  of YBCO film with 0, 5 and 10 mol-% SrTiO<sub>3</sub> nanoparticles. Unfortunately, no pinning effect is observable when the magnetic field is increased, which means that SrTiO<sub>3</sub> nanoparticles do not act as pinning centers. It is also confirmed via the angular dependency at 77 K and 1 T on Figure S9b where no improvement of the pinning effects is shown.

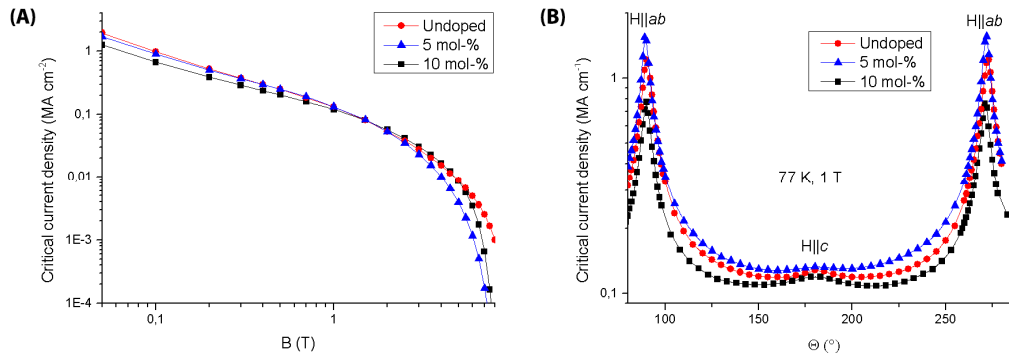


**Figure S9:** Superconducting properties of 5 and 10 mol-% SrTiO<sub>3</sub>-added YBCO nanocomposite films compared with an pristine YBCO film: (A) Magnetic field dependence of critical current density at 77 K and (B) angular dependence of  $J_c$  at 77 K and 1 T.